INFECTION AND IMMUNITY, Oct. 1996, p. 4269–4278 Vol. 64, No. 10
0019-9567/96/$04.00+0

Temporal Analysis of the Developing *Chlamydia psittaci* Inclusion by Use of Fluorescence and Electron Microscopy

DANIEL D. ROCKEY,* ELIZABETH R. FISCHER, AND TED HACKSTADT

Rocky Mountain Laboratories, National Institute of Allergy and Infectious Diseases, Hamilton, Montana 59840

Received 4 March 1996/Returned for modification 23 May 1996/Accepted 23 July 1996

The chlamydiae are obligate intracellular parasites that develop and multiply within a vacuole (termed an inclusion) that does not fuse with lysosomes. Inclusion morphology varies dramatically among the different chlamydiae, particularly within the species *Chlamydia psittaci*. Some strains develop within a single vacuole, while the mature inclusion of other strains consists of several distinct lobes, each filled with chlamydial developmental forms. The development of this lobed structure was investigated in HeLa cells infected with the guinea pig inclusion conjunctivitis (GPIC) strain of *C. psittaci*. We employed two recently described probes for the chlamydial inclusion to study the development of these unique lobed structures. The novel probes were an antiserum directed at a protein localized to the GPIC inclusion membrane (anti-IncA) and the fluorescent sphingolipid {*N*-[7-(4-nitrobenzo-2-oxa-1,3-)]} aminocaproyl sphingosine (NBD-ceramide). Lobed inclusions developed in cells infected at very low multiplicities of infection, suggesting that the structure is not a function of infection by more than one elementary body (EB). Double-label fluorescent-antibody analysis with anti-IncA and an antibody directed at a chlamydial outer membrane protein showed that, prior to 18 h postinfection (p.i.), the inclusion membrane and the chlamydial membrane were tightly associated. After 18 to 20 h p.i., the lobes began to expand and fill with developmental forms and the inclusion membrane and chlamydial membrane became distinct. At times from 8 to 48 h p.i., GPIC inclusions were shown to receive fluorescent derivatives of NBD-ceramide and to be localized to the perinuclear region of the host cell. Labeled lectins with affinity for carbohydrate moieties localized to the Golgi apparatus showed that the lobes of mature inclusions surround the Golgi apparatus. Labeling with NBD-ceramide and the Golgi apparatus-specific lectins therefore demonstrated a functional and physical association of the inclusion with the Golgi apparatus throughout the developmental cycle. Collectively, these results lead to a model for the development of the lobed chlamydial inclusion. We propose that the lobed structure is a result of division of inclusions occurring in parallel with the multiplication of reticulate bodies (RB) early in the developmental cycle. The division of inclusions slows or stops in mid-cycle, and dividing RB accumulate within the enlarging lobes. The RB then differentiate to EBs, the inclusion and cell are lysed, and EBs are freed to infect another cell.

Chlamydiae develop and multiply within intracellular vacuoles, called inclusions, that are not acidified and do not fuse with lysosomes (7, 25). The cellular and molecular processes leading to the development of the inclusion are only beginning to be understood. While there are many similarities among the developmental cycles of the different chlamydial species, significant differences have also been demonstrated. These include differences in inclusion morphology, kinetics of development in tissue culture, contents of the inclusion (i.e., glycogen), and association with cellular organelles (13, 15). For example, *Chlamydia trachomatis*, *C. pneumoniae*, and many strains of *C. psittaci* and *C. pecorum* develop within inclusions consisting of a single vacuole, and inclusions formed in cells infected with multiple elementary bodies (EB) will fuse (3, 13, 16, 18). There are many strains of *C. psittaci*, however, that form multiple, or lobed, inclusions in which fusion of inclusions is apparently limited. The origin and development of these lobed inclusions have not been described beyond an initial biotyping study (22), but it has been proposed that they form as a result of high multiplicities of infection (MOI) (9).

Recently we identified a protein (IncA) of the guinea pig inclusion conjunctivitis (GPIC) strain of *C. psittaci* that is localized to the membrane of the lobes of the inclusion of infected cells (19). Antiserum directed at IncA (anti-IncA) has facilitated the analysis of the developing GPIC inclusion and has allowed the initial characterization of its interaction with host cell components. We have also recently shown that a metabolic product of the fluorescent vital strain {*N*-[7-(4-nitrobenzo-2-oxa-1,3-)]} aminocaproyl sphingosine (NBD-ceramide) is a useful marker for analysis of the cell biology of chlamydial host-pathogen interactions. NBD-ceramide, like endogenous ceramide, is processed to sphingomyelin or glucosylceramide within the Golgi apparatus prior to transport to the plasma membrane via a vesicle-mediated process (11). In cells infected with *C. trachomatis*, the trafficking of Golgi apparatus-derived lipid is interrupted and approximately 50% of the labeled sphingomyelin is instead directed to the developmental forms within the inclusion (5, 6).

In this study, we used these labels to characterize the developing inclusion formed within GPIC-infected cells. The lobed structure of the inclusion was found consistently in HeLa cells infected with GPIC, and lobe formation was independent of MOI. Double-label fluorescence microscopy and electron microscopic analyses of infected cells fixed and stained at different time points postinfection (p.i.) support a model based on the concept that the lobes of the inclusion are formed by division of vacuoles following early division of the GPIC reticulate bodies (RB). Additionally, NBD-ceramide was shown to be trafficked to the GPIC inclusion in a fashion similar to that seen in *C. trachomatis*-infected cells, indicating that the functional connection between the Golgi apparatus and the inclusion is likely common among the chlamydiae (6).

* Corresponding author. Phone: (406) 363-9261. Fax: (406) 363-9204. Electronic mail address: dan_rockey@nih.gov.

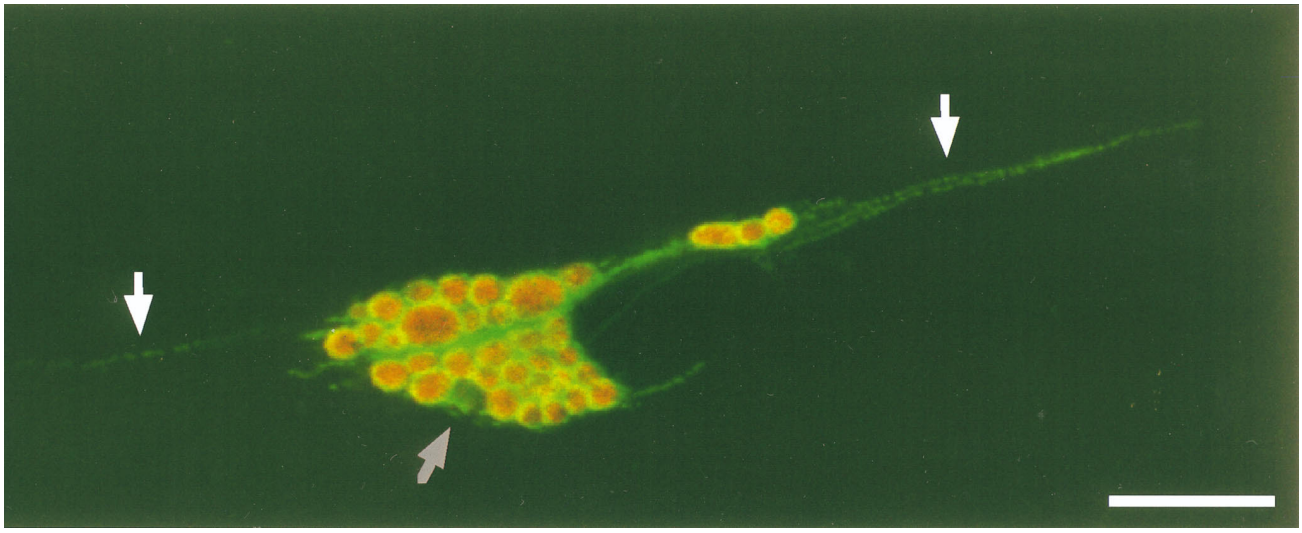

FIG. 1. Double-label fluorescence microscopic image of a mature GPIC inclusion in a HeLa cell. Cells were fixed 36 h p.i. The antibodies used are anti-IncA (green) and anti-MOMP (red). Fibers extending over the nucleus and into the cytoplasm of the cell are indicated with white arrows, and an empty lobe is indicated with a grey arrow. MOI, approximately 0.01. Bar, 10 μm.

MATERIALS AND METHODS

Antibodies and reagents. Production of antiserum specific to the *C. psittaci* IncA protein has been described previously (19). Monoclonal antibody to *C. psittaci* GPIC major outer membrane protein (MOMP) was a gift from You-Xun Zhang of the Maxwell Findland Laboratory, Boston, Mass. All fluorescence-labeled second antibodies were obtained commercially (U.S. Biochemical Corporation, Cleveland, Ohio). The fluorescent vital stain NBD-ceramide was purchased from Molecular Probes (Eugene, Oreg.). Calcium- and magnesium-free Hanks' balanced salt solution (HBSS) (catalog no. 14170) was purchased from Gibco/BRL (Gaithersburg, Md.).

Chlamydial culture and fixation procedures. *C. psittaci* GPIC was obtained from Roger Rank, University of Arkansas at Little Rock. *C. trachomatis* LGV-434 (serovar L2) was acquired from the American Type Culture Collection (Rockville, Md.). All cell culture was performed with HeLa cells incubated in minimum essential medium plus 10% fetal calf serum (MEM-10; Gibco/BRL). Monolayers of HeLa cells grown on sterile 12-cm-long coverslips were infected

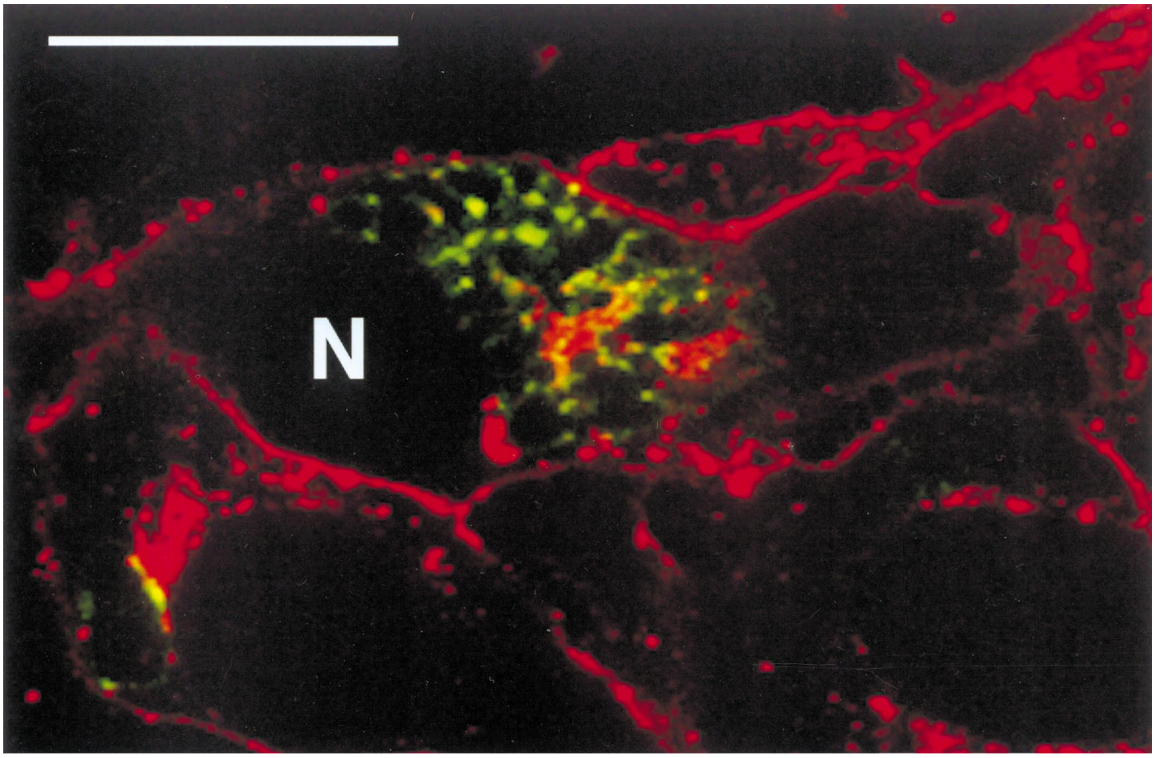

FIG. 9. Confocal micrograph of a *C. psittaci* GPIC inclusion (36 h p.i.) in a HeLa cell labeled with anti-IncA (green label) and lectin WGA (red label). Cells were infected at MOI of 0.5 to 1.0. WGA has affinity for carbohydrate moieties located in the Golgi apparatus and on the plasma membrane. The orange staining within the center of the inclusion is a region brightly labeled with both anti-IncA and WGA. Bar, 10 μm. N, nucleus.

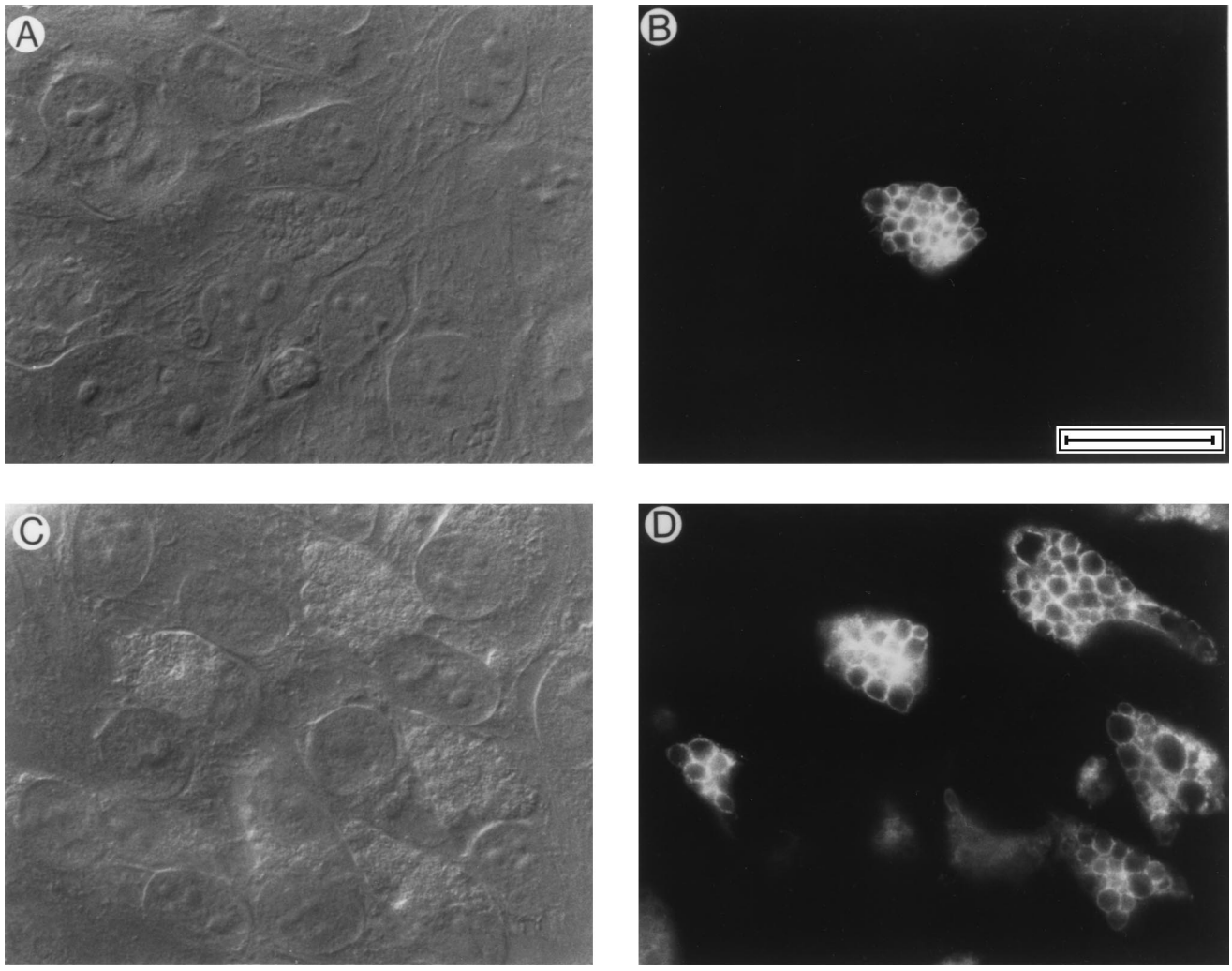

FIG. 2. Differential interference contrast (A and C) and fluorescent images (B and D) of mature inclusions formed in cells infected at an MOI of 0.001 (A and B) and at an MOI of approximately 0.5 (C and D). Cells were fixed 36 h p.i. and labeled with anti-IncA. Bar, 10 μm.

with GPIC or LGV-434 at the MOI indicated in the figure legends. EB used for all infections were purified by the methods of Caldwell et al. (2), divided into aliquots, and stored at −70°C. Chlamydiae were diluted in cold SPG (0.25 M sucrose, 10 mM sodium phosphate, 5 mM L-glutamic acid [pH 7.2]) prior to infection. Cells were incubated for 1 h at room temperature, with rocking, prior to removal of inocula and addition of prewarmed MEM-10. Infected cells were incubated at 37°C in a humidified 5% CO_2 environment. Following culture, cells were fixed with 100% methanol for 5 min and stored in HBSS at 4°C.

***C. psittaci* growth curve.** HeLa cells were infected in 24-well trays and lysed after selected time intervals from 0 to 40 h p.i. At each time point cells were washed with HBSS and incubated in 0.5 ml of water for 1 min to lyse the host cells. An equal volume of SPG was then added to the well, the contents were mixed, and the lysate was removed and stored at −70°C. After all samples were collected, the lysates were thawed and the output inclusion-forming units were determined for each time point. The lysates were diluted, inoculated in triplicate onto HeLa cells in 48-well plates, cultured in MEM-10 for 40 h, and methanol fixed. Chlamydial inclusions within these monolayers were labeled with antibody as described below, and the numbers of inclusions in 10 fields from each of the triplicate wells were counted. These values were converted to infectious EB per milliliter of the lysate collected at each of the time points on the growth curve.

Labeling of cells with fluorescent probes. Fixed cells used in immunofluorescence were blocked with 2% bovine serum albumin in phosphate-buffered saline (BSA-PBS) for 5 min at RT. Antibodies diluted in BSA-PBS were added, and mixtures were incubated at RT for 1 h. Coverslips were washed three times with PBS, and appropriate second antibodies (diluted 1/1,000 in BSA-PBS) were added. Second antibodies were incubated on cells for 1 h at RT, and then the wells were washed three times with PBS. Coverslips were removed and inverted onto a microscope slide in a drop of antibleaching agent (Vectashield; Vector Laboratories, Burlingame, Calif.).

Live GPIC- and L2-infected HeLa cells were labeled with NBD-ceramide by methods described by Hackstadt et al. (6), with minor modifications. Briefly, infected cells were washed with HBSS and incubated 15 min at 37°C with NBD-ceramide complexed to 0.034% defatted BSA in MEM. The concentration of both NBD-ceramide and defatted BSA was approximately 5 μM. Cells were then washed with HBSS and incubated for 1 h at 37°C in MEM plus 0.34% defatted BSA. Cells were washed with HBSS and examined by conventional or confocal microscopy.

Wheat germ agglutinin (WGA) is a lectin with specificity for glycoproteins localized to the Golgi apparatus and plasma membrane (23). To reduce staining of the plasma membrane by Texas red-WGA, the surfaces of paraformaldehyde-fixed, infected HeLa cells were blocked with unlabeled WGA (25 μg/ml of HBSS) for 30 min prior to permeabilization with methanol. Cells were then incubated in anti-IncA for 1 h, washed, and incubated in fluorescein-labeled anti-rabbit antisera plus Texas red-labeled WGA (25 μg/ml of HBSS). After 1 h, cells were washed and visualized by confocal microscopy.

Fluorescence and confocal microscopy. Conventional fluorescence microscopy was conducted on a Nikon Microphot FXA microscope by using a 60× objective and oil immersion. Photographs were taken on the Microphot microscope with 400 ASA Elite or Tmax film (Eastman Kodak, Rochester, N.Y.). Digital images were collected by using a Dage-MTI CCD-72 camera and recorded with a DSP-2000 image processor (Dage-MTI Inc., Michigan City, Ind.). Confocal microscopy was conducted on an MRC-1000 confocal imaging system equipped with a krypton-argon laser (Bio-Rad Laboratories, Hercules, Calif.) with a Zeiss Axiovert 135 inverted microscope, by using a 63× Planapochromat objective and

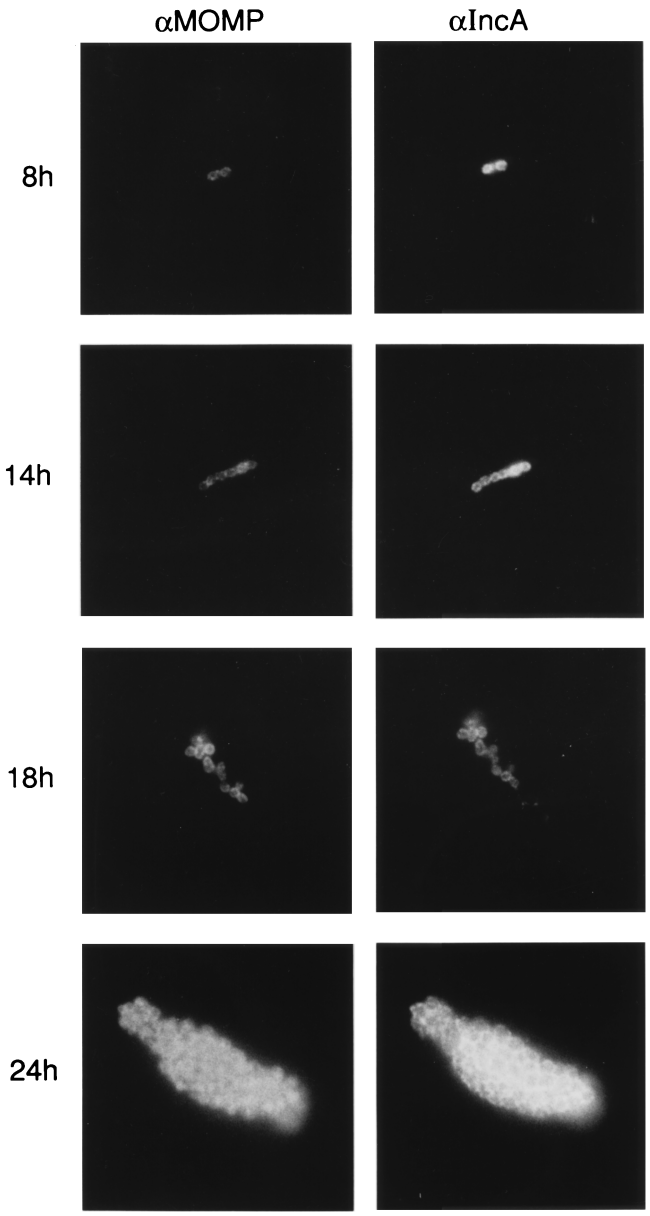

FIG. 3. Temporal analysis of inclusion development by fluorescence microscopy of fixed, infected HeLa cells. HeLa cells were infected with GPIC at an MOI of less than 0.01 and fixed with methanol at selected times p.i. Coverslips were double labeled with anti-IncA (αIncA) and anti-MOMP (αMOMP) monoclonal antibody and viewed by fluorescence microscopy.

oil immersion. All images collected electronically were processed by using Adobe Photoshop 2.5.1 (Adobe Systems, Mountain View, Calif.) and printed on a Phaser 440 dye sublimation printer (Tektronix, Wilsonville, Oreg.).

Video images of GPIC-infected HeLa cells were collected and recorded on videotape in real time. Coverslips with live infected cells (48 h p.i.) were inverted onto a drop of MEM-10 and viewed on the Nikon Microphot FXA microscope by using Nomarski differential interference contrast microscopy. Individual frames were digitized by using Comos image analysis software (Bio-Rad) and processed in Adobe Photoshop.

Electron microscopy. Transmission electron microscopy was conducted by using the methods of McDonald (14), with the following modifications. HeLa cells were grown on Thermanox coverslips (Nunc, Inc., Naperville, Ill.) prior to infection with GPIC at an MOI of less than 1. Cultures were incubated for time intervals of 8 to 48 h prior to being washed twice with cold 100 mM cacodylate buffer, pH 7.4. Infected cells were then fixed at 4°C for 2 h in 4% paraformaldehyde–2.5% glutaraldehyde in 100 mM cacodylate buffer, pH 7.4. Cells were postfixed in 0.5% OsO_4–0.8% $K_3Fe(CN)_6$ followed by 1% tannic acid and stained overnight en bloc in 1% uranyl acetate. Samples were dehydrated in a graded ethanol series and embedded in Spurr's resin. Thin sections were cut with an MT-7000 ultramicrotome (Research and Manufacturing Company, Inc., Tucson, Ariz.), stained with 1% uranyl acetate and Reynold's lead citrate (17), and observed at 80 kV on a Philips CM-10 transmission electron microscope (Philips, Eindhoven, The Netherlands).

RESULTS

Fluorescence microscopic analysis of the GPIC inclusion. The mature GPIC inclusion is a lobed structure, and virtually every lobe is densely packed with developmental forms. Double-label fluorescence microscopy of fixed, infected HeLa cells demonstrated that IncA is localized to the margins of the lobes, while MOMP is localized to the developmental forms within the lobes (Fig. 1) (19). IncA-laden lobes that did not contain EB or RB were also occasionally observed (Fig. 1). We examined the development of the lobed inclusion by comparing the inclusion formation at an MOI of less than 0.01 with that of cells infected at higher MOI. Direct counts of GPIC developmental forms in cells infected at very low MOI were conducted 6 h p.i. to verify that more than 80% of infected cells contained single bacteria. At any MOI examined the lobed structures of the inclusions were similar, and the number of lobes did not increase with increasing MOI (Fig. 2). This result demonstrated that the formation of the lobed inclusion was independent of MOI; therefore, the development of lobed or multiple inclusions was not simply a result of the inability of multiple GPIC inclusions to fuse. Instead, this suggested that the lobed structure formed following division of inclusions during the developmental process.

The temporal development of the GPIC inclusion was examined by fluorescence microscopic analysis of infected cells fixed at different times p.i. For these experiments, cells were again infected at MOI of less than 0.01. Examination of cells 8 to 20 h p.i. demonstrated that early in the infectious process, anti-MOMP and anti-IncA staining colocalized at the margin of the inclusion and the surface of the developmental form (Fig. 3, 8 to 18 h), suggesting the vacuolar and chlamydial membranes were tightly juxtaposed. This staining pattern was consistent until after 18 to 20 h p.i., when the structure of the inclusion began to change. At 24 h p.i. (Fig. 3, 24 h) and at all later time points (Fig. 1 and 2), staining with these antibodies demonstrated that the margins of the inclusion and the individual developmental forms were distinct. The individual lobes became larger, and the numbers of RB in each lobe increased. The result of this development was an inclusion consisting of many individual vacuoles filled with numerous developmental forms. Because each infection was initiated by a single EB, the lobed inclusion was a result of division of inclusions as the bacteria within the cell divide.

Ultrastructural analysis of the GPIC inclusion. Electron microscopy of infected cells at selected times p.i. demonstrated that inclusion morphologies were distinct at different stages of development (Fig. 4). At 8 h p.i. the infecting chlamydiae have differentiated from EB to RB, as evidenced by increased size and dispersal of condensed chromatin, but minimal bacterial division has occurred (Fig. 4A). Micrographs of cells fixed 13 to 18 h p.i. revealed pleomorphic RB and an irregular inclusion structure. In these images it was commonly difficult to distinguish the inclusion membrane from the RB membrane, or to visualize complete membranes around individual RB (Fig. 4B and C). Examination of cells fixed 22 h p.i. showed that the inclusion and the RB are more clearly distinguishable and that the developmental forms have begun to dedifferentiate back to EB (Fig. 4D and E). This time point also corresponds to the first period that culturable EB can be harvested from the

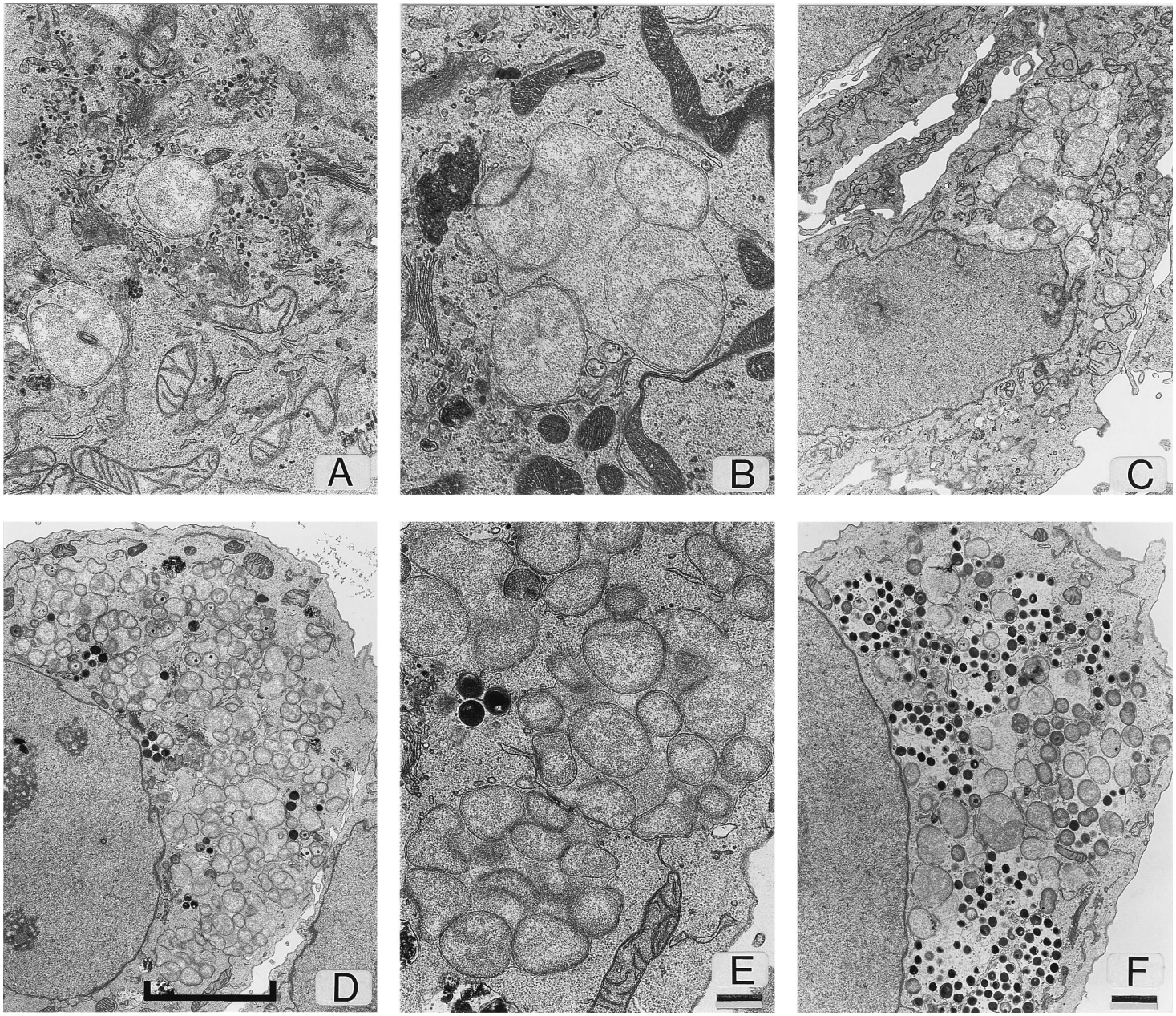

FIG. 4. Temporal analysis of the ultrastructure of the developing GPIC inclusion. HeLa cells were infected with GPIC and fixed at 8 (A), 13 (B), 18 (C), 22 (D and E), or 48 (F) h p.i. Panel E is a higher magnification of the area above the bracket in panel D. Cells shown in panel A were infected at MOI of about 1. All other panels show cells infected at MOI less than 0.1. (E) Bar, 1.6 μm (for panels A, B, and E), (F) bar, 0.5 μm (for panels C, D, and F).

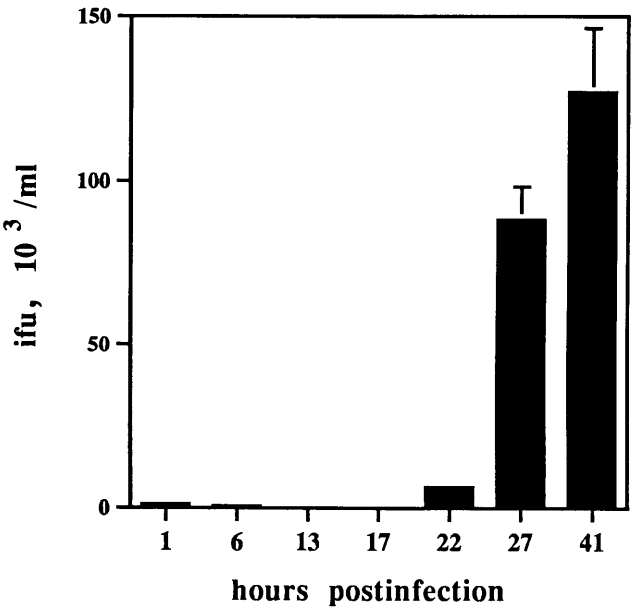

FIG. 5. Development of culturable EB in HeLa cells infected with *C. psittaci* GPIC. Infected cells were lysed with water at the indicated times p.i., and the lysates were replated to new HeLa cells in triplicate. These cells were incubated 40 h, and then the inclusion-forming units (ifu) in these cells were counted. The data represent ifu per milliliter of lysate; bars, one standard error.

developing inclusions (Fig. 5). The number of infectious EB rises dramatically in the next 8 h, a time interval in which the lobes expand considerably. Therefore, a change in the structure of the inclusion, as determined by fluorescence and electron microscopy, is associated with the changing developmental cycle of the chlamydiae within the inclusion.

Characterization of the late GPIC inclusion. Throughout the course of the infectious cycle the developmental forms within the GPIC inclusion are densely packed and do not display the vigorous Brownian motion characteristic of EB in *C. trachomatis* inclusions. However, very late in the GPIC infectious cycle the inclusions degenerate and EB flow freely within the lobes and the cytoplasm of infected cells. Electron micrographs taken at 48 h p.i. demonstrated that the inclusion structure was very large and many lobes appeared to be lysing (Fig. 4F). Microscopic analysis of live infected cells 48 h p.i. confirmed that many EB are free in the cytoplasm, with some lobe structure remaining in the degenerating cell. The lobes appeared independent of one another. In a single case we photographed an intact lobe leaving a degenerating infected cell (Fig. 6). Over the course of approximately 0.5 s, the lobe burst through the plasma membrane, followed by a stream of cytoplasmic material and large numbers of free EB. The lobe remained intact and associated with the surface of the cell, at the point of extrusion, over the course of the viewing period (several minutes).

The interaction of GPIC inclusions with the Golgi apparatus. *C. psittaci* GPIC-infected HeLa cells were labeled with NBD-ceramide to determine if *C. psittaci* inclusions similarly interrupted sphingolipid export. Incorporation of NBD-ceramide by GPIC developmental forms was apparent at any tested time point (Fig. 7), and trafficking of the fluorescent analog to the inclusion and incorporation by the intracellular chlamydial developmental forms were similar to what was observed for *C. trachomatis* (Fig. 8). Chlamydial developmental forms were labeled in every lobe examined, indicating that the NBD-ceramide was uniformly trafficked to each lobe. This result demonstrated a functional association of the developing GPIC inclusion with the host cell Golgi apparatus.

The images in Fig. 8 also show the distinct structural differences between the mature inclusions of *C. trachomatis* and *C. psittaci* GPIC. Whereas the *C. trachomatis* inclusion is a single large vacuole containing multiple chlamydial developmental forms, the *C. psittaci* inclusion is clearly multilobed with the fluorescence-labeled chlamydiae localized to discrete clusters. Also apparent in GPIC-infected cells is a proportion of the fluorescent probe in fibers that are morphologically similar to those previously described as containing IncA (Fig. 1) (19). We are currently investigating the possibility that the ceramide-containing fibers are also laden with IncA.

A structural association of the *C. psittaci* inclusion and the Golgi apparatus was shown by confocal microscopic analysis of infected cells labeled with antibodies and Golgi apparatus-specific lectins. The photomicrograph in Fig. 9 represents fixed and permeabilized *C. psittaci*-infected HeLa cells (36 h p.i.) labeled with anti-IncA and the lectin WGA. This lectin has specificity for carbohydrate moieties found on proteins in the Golgi apparatus and the plasma membrane (23). Late inclusions, such as those shown in Fig. 9, generally surround the Golgi apparatus, with intense anti-IncA staining always localized with the brightest staining by labeled WGA. Early *C. psittaci* inclusions (10 to 20 h p.i.) are generally positioned adjacent to and in contact with the Golgi apparatus (data not shown).

DISCUSSION

The results described above demonstrate that infection with *C. psittaci* GPIC results in a distinct inclusion morphology consisting of multiple, independent vacuoles localized in the perinuclear region of the cell. This lobed structure develops even after infection at very low MOI, implying that the lobes increase in number during the course of GPIC multiplication.

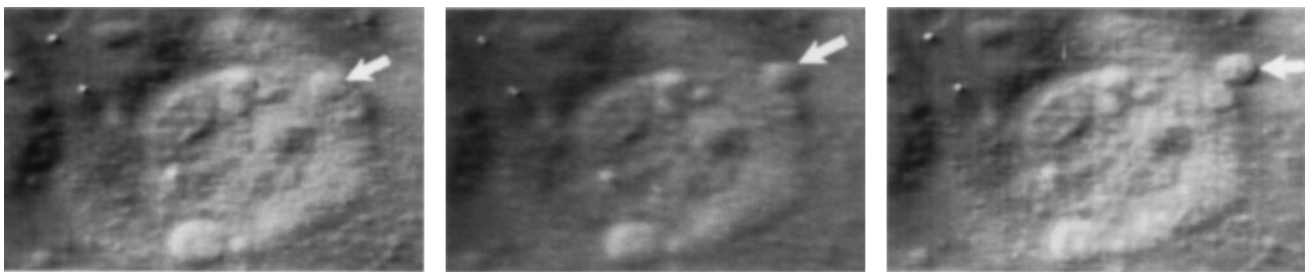

FIG. 6. Differential interference contrast video microscopy of a GPIC inclusion in a HeLa cell 48 h p.i. The three images were collected in real time over the course of less than 1 s. The arrows point to a single lobe that escapes from the cell.

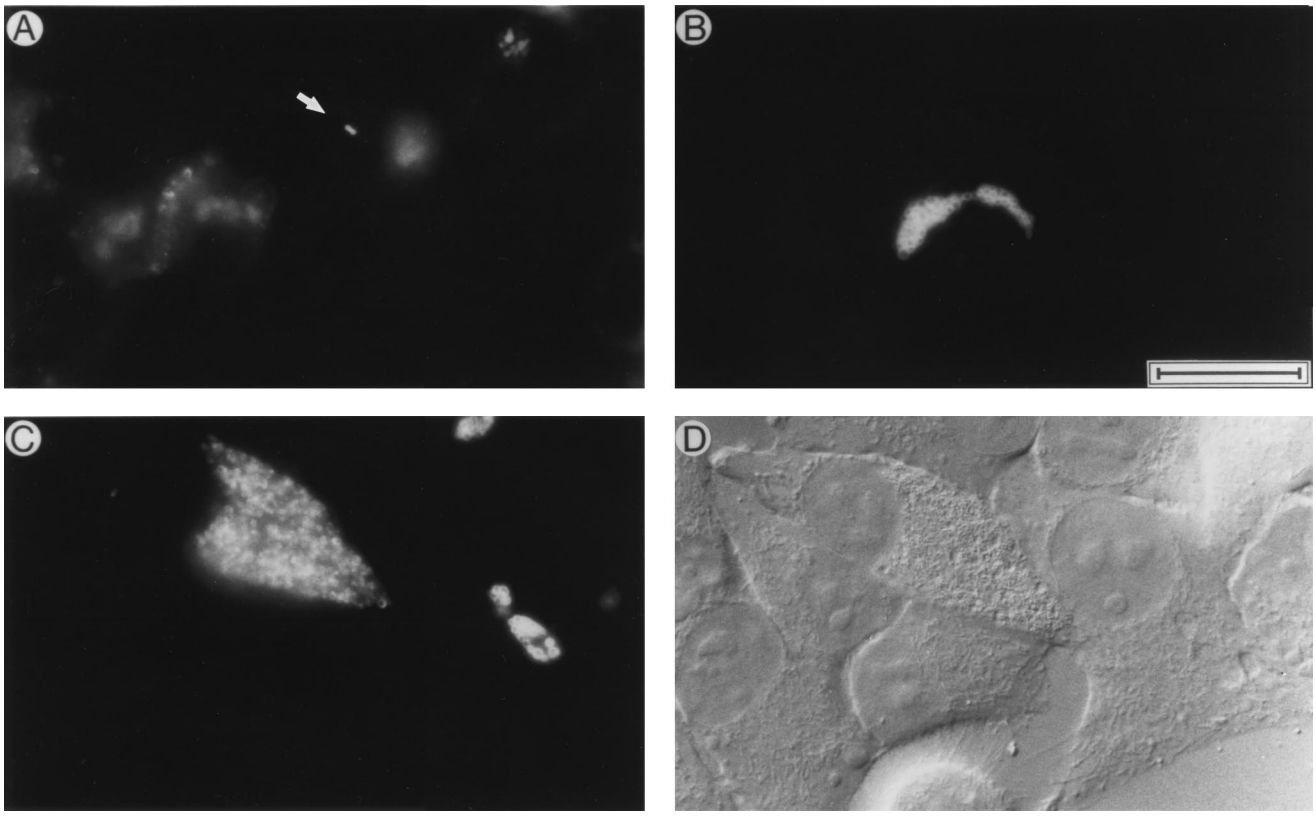

FIG. 7. Uptake by *C. psittaci* GPIC of the Golgi apparatus-specific vital stain NBD-ceramide at selected points in the developmental cycle. Infected cells were labeled with NBD-ceramide at 8 (A), 18 (B), and 44 (C and D) h and visualized by conventional fluorescence microscopy. (A) The arrow points to the two developmental forms. (D) Differential interference contrast image of the labeled cell shown in panel C. Bar, 10 μm.

Additionally, the inclusion communicates with the Golgi apparatus throughout the developmental cycle and each lobe of the mature inclusion interacts with Golgi apparatus-derived vesicles. Double-label fluorescent-antibody analysis with anti-IncA and lectins specific for the Golgi apparatus demonstrates a physical association as well, with early inclusions lying adjacent to the Golgi apparatus (data not shown) and terminal inclusions surrounding the Golgi apparatus (Fig. 9). We have used the images presented in this paper to develop a model for the formation of the lobed GPIC inclusion (Fig. 10). In the following section we describe this model and contrast GPIC development with the well-characterized developmental cycle of *C. trachomatis.*

C. trachomatis EB are delivered to the perinuclear region and begin to acquire sphingolipids from the host cell by 2 h p.i. (5). Similarly, we show here that *C. psittaci* EB quickly arrive at a similar site and remain associated with the Golgi apparatus for the entirety of their developmental cycle. The EB differentiate and begin to divide approximately 6 to 8 h p.i. Both fluorescence microscopy (Fig. 3) and labeling with NBD-ceramide (Fig. 7) suggest that early division of GPIC RB may proceed through classical binary fission. This is consistent with compelling ultrastructural data derived from other chlamydiae (1, 4, 8, 10, 12) in which dividing RB are common. In our experimentation, however, it was not possible to identify, in inclusions up to 22 h p.i., ultrastructural evidence for binary fission of GPIC. It was apparent that the size of the inclusion and numbers of developmental forms were both increasing, but we found no representative images of classical bacterial division. Our inability to detect such dividing bacteria may have been a result of a sample preparation artifact or of limitations associated with the thin-sectioning process, but we cannot rule out the possibility that a different multiplication scheme may be used during GPIC development. In a model similar to that discussed briefly by Ward (24), multiple chromosomes might be synthesized within an enlarging RB, surrounded by a tightly opposed inclusion membrane. Inner and/or outer membranes, still linked to developing inclusion membrane, might then form septae around individual nucleoid centers. The result of this would be multiple RB progeny from a single parent RB, each surrounded by its own inclusion membrane.

Our model suggests that the inclusion membrane remains tightly associated with RB during the first half of the developmental cycle. This hypothesis is based on the circumferential staining of IncA around each of the progeny RB prior to 20 h p.i. We propose that during this phase of development the inclusion membrane segregates in conjunction with fission of the chlamydiae. Such a mechanism would provide for the increase in the number of lobes in the mature inclusion in cells infected at low MOI. However, it is apparent that the division of inclusions in concert with RB multiplication occurs only for a limited period and at some point the RB begin to accumulate within growing lobes. Fluorescence and electron microscopy data suggest that this change occurs approximately 20 to 22 h p.i., just prior to the period of rapidly increasing numbers of infectious EB in the culture. It is possible that developmental signals responsible for the differentiation of EB to RB are also associated with the changing structure of the inclusion.

By 20 h p.i., inclusion development apparently enters a new phase. Fluorescence microscopy demonstrated that after this

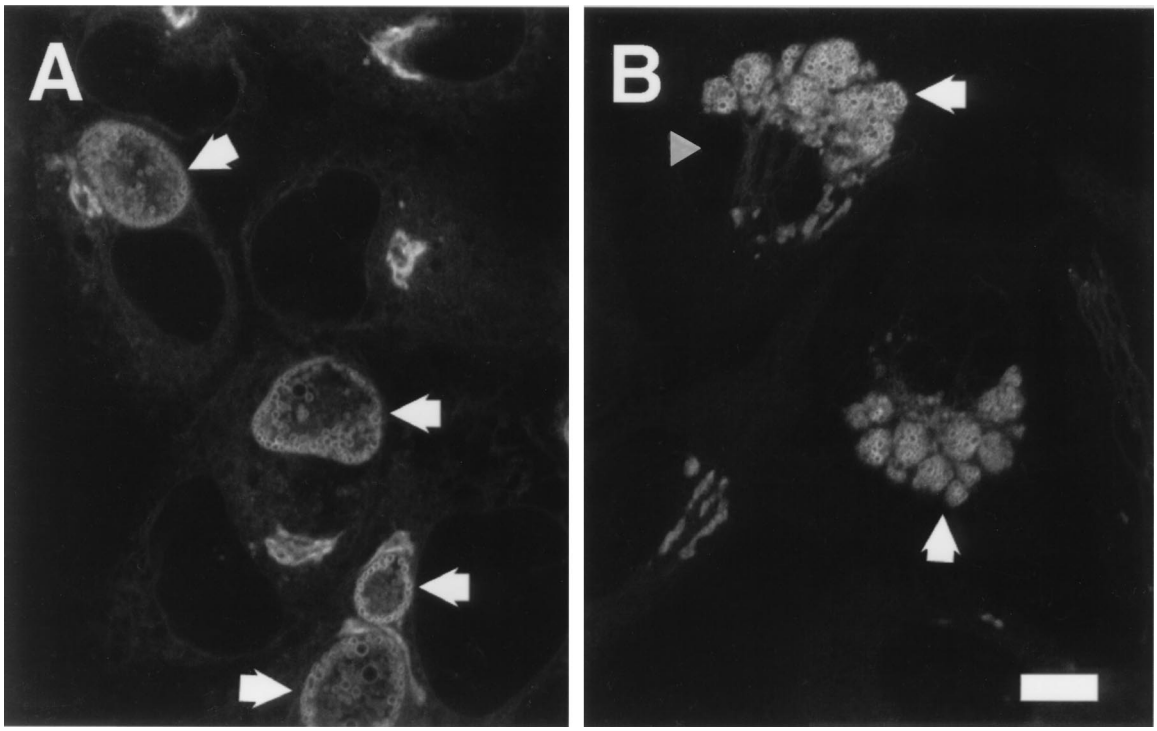

FIG. 8. *C. trachomatis* LGV-434 (A) and *C. psittaci* GPIC (B) inclusions in HeLa cells labeled with NBD-ceramide. Cells were infected at an MOI of 0.5 and were labeled 24 h p.i. Arrows point to the inclusions, and NBD-ceramide-labeled fibers in the GPIC-infected cells are indicated with an arrowhead. Bar, 10 μm.

time point, the IncA in the inclusion membrane is clearly resolved from MOMP in the chlamydial outer membrane. By electron microscopy, the membranes of the inclusion and the RBs are readily distinguished and the lobes of the inclusion are apparent. This period precedes the major differentiation of RB to EB, as is evident in electron micrographs and from the culture data. Developmental forms are still tightly packed within these lobes, in contrast to the more spacious and refractile inclusion formed in *C. trachomatis*-infected cells at similar time points (Fig. 8). This developmental step does not appear to be synchronous in all lobes, suggesting that the environmental signal for differentiation may not be received by all lobes simultaneously.

The model predicts that terminal differentiation of RB to EB follows the change in the structure of the inclusion witnessed between 18 and 24 h p.i. Terminal differentiation accelerates over the period from 24 to 30 h, inclusions begin to lyse in the cell, and free EB accumulate within the cytoplasm. While we did observe a lobe escaping from a degenerating cell, it is apparent that this was a rare event—most of the lobes are lysed prior to lysis of the cell. The last step in development is lysis of the cell, allowing EB to infect another cell and start the cycle again.

In this work, we used fluorescence and electron microscopy to characterize the development of the unusual lobed inclusion characteristic of *C. psittaci* GPIC. Collectively, the photomicrographs demonstrate the differences between the developmental cycles of GPIC, an example of a chlamydial strain that occupies lobed inclusions, and *C. trachomatis* LGV-434 (serovar L2), an example of a chlamydial strain that develops within a single inclusion. Although this is the first detailed characterization of a lobed chlamydial inclusion, this is not because few chlamydiae share this trait with GPIC. Spears and Storz (22) developed a biotyping scheme for classification of *C. psittaci* based on inclusion morphology. Photomicrographs of seven of the eight biotypes show lobed or multiple inclusions within infected cells. In their analysis of 29 *C. psittaci* strains, Spears and Storz placed 17 independent strains into biotypes with lobed inclusions. Although these experiments may be complicated somewhat by the likelihood that cells were infected at high MOI, they establish that the lobed inclusion is a structure common to many different *C. psittaci* strains. Included in this group are isolates causing clinical conditions in a variety of domestic animal species.

Many questions arise regarding the selective advantage or disadvantage of the lobed inclusion and regarding the molecular mechanisms leading to this unique structure. An example of how the lobed inclusion may be a benefit to the pathogen is in its greater surface area in contact with the cytoplasm. This may allow some selective advantage in the acquisition of nutrients from the cytoplasm or allow for the availability of more sites for docking with Golgi apparatus-derived vesicles. Molecular mechanisms that cause the described difference in inclusion structure are unknown. It is possible that the lobed inclusion is a result of differences in the spectrum of proteins inserted by chlamydiae into the inclusion membrane (19, 20). These differences may facilitate slightly different interactions with host cell cytoskeletal components, resulting in differences in inclusion structure. Support for this premise comes from work with cytoskeletal inhibitors of *C. trachomatis*-infected cells. Inhibition of microtubule or microfilament structure or function early in the developmental cycle eliminates the ability of *C. trachomatis* serovar L2 inclusions to fuse but does not affect the fusogenic nature of serovar E inclusions (21). This inhibition leads to multiple *C. trachomatis* L2 inclusions in cells infected at MOI greater than 1, a structure superficially similar to the lobed GPIC inclusion. It is likely that the lobed inclusions produced during GPIC infection are less fusogenic than

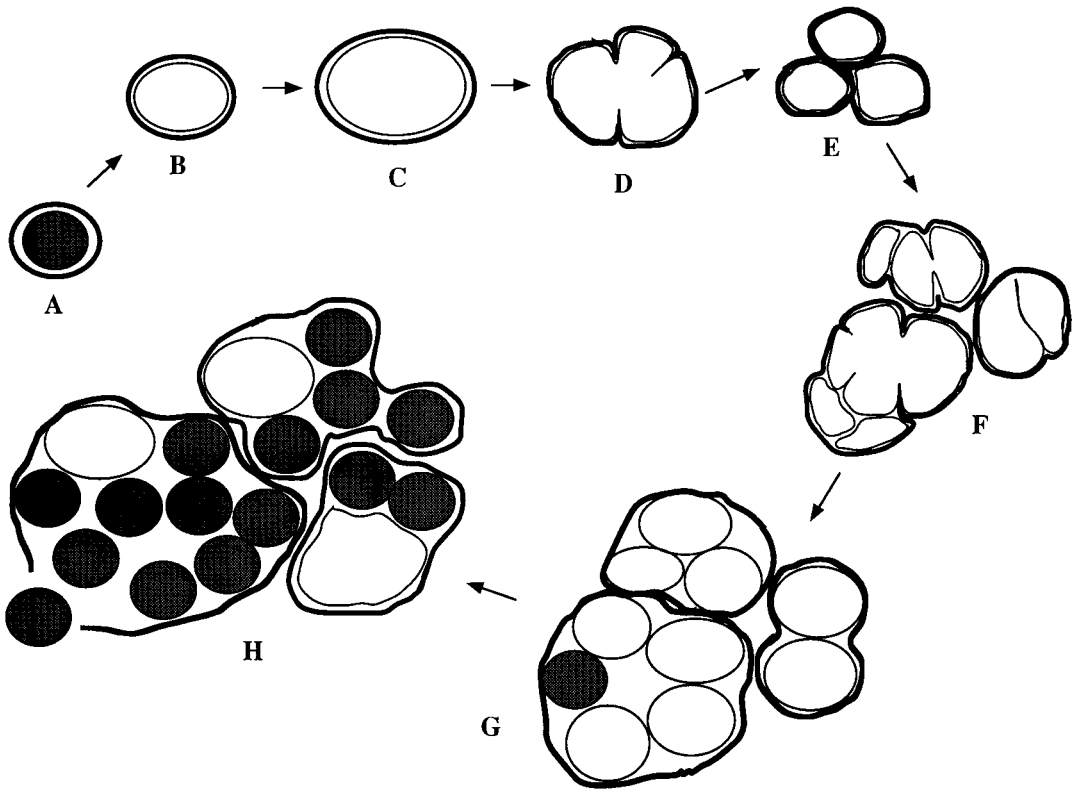

FIG. 10. Model of the development of the lobed chlamydial inclusion. The model begins with the EB (filled circle) inside an early inclusion within the infected cell (A). The EB differentiates to an RB (open oval) which then grows and multiplies within the growing inclusion (B to D). The inclusion membrane (thick lines) grows with the growing bacterial membrane, and multiplication of RB leads to the formation of new lobes of the inclusion (E). A second round of RB enlargement may follow, yielding more RB, each enclosed in a new lobe. After approximately 20 h, differentiation of RB back to EB commences cotemporally with the accumulation of developmental forms within each lobe (F to G). Differentiation then proceeds, the inclusion and the cell are lysed, and EB are freed to infect another cell (H).

uninhibited *C. trachomatis* inclusions. This difference therefore may be a result of differences in the interaction of the inclusion surface with cytoskeletal components. We anticipate that a further understanding of the host-pathogen interactions involved with the development of these distinct inclusions will facilitate our understanding of the complex intracellular existence of the chlamydiae.

ACKNOWLEDGMENTS

We thank Harlan Caldwell, Witold Cieplak, Robert Heinzen, and Marci Scidmore for editorial assistance in the preparation of the manuscript. Jim Simmons, Gary Hettrick, and Bob Evans provided valuable technical assistance in this work.

REFERENCES

1. **Anderson, D. R., H. E. Hops, M. F. Barile, and B. C. Bernheim.** 1965. Comparison of the ultrastructure of several rickettsiae, ornithosis virus, and *Mycoplasma* in tissue culture. J. Bacteriol. **90:**1387–1403.
2. **Caldwell, H. D., J. Kromhout, and J. Schachter.** 1981. Purification and partial characterization of the major outer membrane protein of *Chlamydia trachomatis*. Infect. Immun. **31:**1161–1176.
3. **Campbell, S., S. J. Richmond, and P. Yates.** 1989. The development of *Chlamydia trachomatis* inclusions within the host eukaryotic cell during interphase and mitosis. J. Gen. Microbiol. **135:**1153–1165.
4. **Friis, R. R.** 1972. Interaction of L cells and *Chlamydia psittaci*: entry of the parasite and host response to its development. J. Bacteriol. **110:**706–721.
5. **Hackstadt, T., D. D. Rockey, R. A. Heinzen, and M. A. Scidmore.** 1996. *Chlamydia trachomatis* interrupts an exocytic pathway to acquire endogenously synthesized sphingomyelin in transit from the Golgi apparatus to the plasma membrane. EMBO J. **15:**964–977.
6. **Hackstadt, T., M. A. Scidmore, and D. D. Rockey.** 1995. Lipid metabolism in *Chlamydia trachomatis* infected cells: directed trafficking of Golgi-derived sphingolipids to the chlamydial inclusion. Proc. Natl. Acad. Sci. USA **92:** 4877–4881.
7. **Heinzen, R. A., M. A. Scidmore, D. D. Rockey, and T. Hackstadt.** 1996. Lysosomal glycoproteins and the vacuolar-type (H+)-ATPase differentiate the parasitophorous vacuoles of *Coxiella burnetii* and *Chlamydia trachomatis*. Infect. Immun. **64:**796–809.
8. **Higashi, N.** 1965. Electron microscopic studies on the mode of reproduction of trachoma virus and psittacosis virus in cell culture. Exp. Mol. Pathol. **4:**24–39.
9. **Hodinka, R. L., C. H. Davis, J. Choong, and P. B. Wyrick.** 1988. Ultrastructural study of endocytosis of *Chlamydia trachomatis* by McCoy cells. Infect. Immun. **56:**1456–1463.
10. **Lepinay, A., J. Orfila, A. Anteunis, J. M. Boutry, L. Orme-Roselli, and R. Robineaux.** 1970. Etude en microscopie electronique du developpement et de la morphologie de *Chlamydia psittaci* dans les macrophages de souris. Ann. Inst. Pasteur **119:**222–231.
11. **Lipsky, N. G., and R. E. Pagano.** 1985. Intracellular translocation of fluorescent sphingolipids in cultured fibroblasts: endogenously synthesized sphingomyelin and glucocerebrocide analogues pass through the Golgi apparatus en route to the plasma membrane. J. Cell Biol. **100:**27–34.
12. **Matsumoto, A.** 1988. Structural characteristics of chlamydial bodies, p. 21–46. *In* A. L. Barron (ed.), Microbiology of Chlamydia. CRC Press, Boca Raton, Fla.
13. **Matsumoto, A., I. Bessho, K. Uehira, and T. Suda.** 1991. Morphological studies of the association of mitochondria with chlamydial inclusions and the fusion of chlamydial inclusions. J. Electron Microsc. **40:**356–363.
14. **McDonald, K.** 1984. Osmium ferricyanide fixation improves microfilament preservation and membrane visualization in a variety of animal cell types. J. Ultrastruct. Res. **86:**107–118.
15. **Moulder, J. W.** 1991. Interaction of chlamydiae and host cells in vitro. Microbiol. Rev. **55:**143–190.
16. **Patton, D. L., and C. C. Kuo.** 1990. Cinematographic observations of growth of *Chlamydia pneumoniae* in primary cultures of monkey conjunctival and human amniotic epithelial cells, p. 20–23. *In* W. R. Bowie et al. (ed.), Chlamydial infections. Cambridge University Press, Cambridge.
17. **Reynolds, E. S.** 1963. The use of lead citrate at high pH as an electron-opaque stain in electron microscopy. J. Cell Biol. **17:**208–213.
18. **Ridderhof, J. C., and R. C. Barnes.** 1989. Fusion of inclusions following

superinfection of HeLa cells by two serovars of *Chlamydia trachomatis*. Infect. Immun. **57:**3189–3193.
19. **Rockey, D. D., R. A. Heinzen, and T. Hackstadt.** 1995. Cloning and characterization of a *Chlamydia psittaci* gene coding for a protein localized in the inclusion membrane of infected cells. Mol. Microbiol. **15:**617–626.
20. **Rockey, D. D., and J. L. Rosquist.** 1994. Protein antigens of *Chlamydia psittaci* present in infected cells but not detected in the infectious elementary body. Infect. Immun. **62:**106–112.
21. **Schramm, N., and P. B. Wyrick.** 1995. Cytoskeletal requirements in *Chlamydia trachomatis* infection of host cells. Infect. Immun. **63:**324–332.
22. **Spears, P., and J. Storz.** 1979. Biotyping of *Chlamydia psittaci* based on inclusion morphology and response to diethylaminoethyl-dextran and cycloheximide. Infect. Immun. **24:**224–232.
23. **Virtanen, I., P. Ekblom, and P. Laurila.** 1980. Subcellular compartmentalization of saccharide moieties in cultured normal and malignant cells. J. Cell Biol. **85:**429–434.
24. **Ward, M. E.** 1983. Chlamydial classification, development and structure. Br. Med. Bull. **39:**109–115.
25. **Wyrick, P. B., and E. A. Brownridge.** 1978. Growth of *Chlamydia psittaci* in macrophages. Infect. Immun. **19:**1054–1060.

Editor: A. O'Brien